Science of the Total Environment 822 (2022) 153600

Contents lists available at ScienceDirect

Science of the Total Environment

journal homepage: www.elsevier.com/locate/scitotenv

An integrated approach combining magnetic, geochemical and particle-based techniques to assess metal(loid) loadings in urban venues frequented by children

A. Bourliva [a,b,*], E. Aidona [b], L. Papadopoulou [c], E. Ferreira da Silva [d], C. Patinha [d], C. Sarafidis [e], N. Kantiranis [c]

[a] Chemical Process and Energy Resources Institute, Centre for Research and Technology Hellas-CERTH, 6th km Charilaou-Thermi Rd, 57001 Thessaloniki, Greece
[b] Department of Geophysics, School of Geology, Aristotle University of Thessaloniki, 54124 Thessaloniki, Greece
[c] Department of Mineralogy-Petrology-Economic Geology, School of Geology, Aristotle University of Thessaloniki, 54124 Thessaloniki, GREECE
[d] GeoBioTec, Department of Geoscience, University of Aveiro, Campus de Santiago, 3810-193 Aveiro, Portugal
[e] Laboratory of Physics, Department of Physics, Aristotle University of Thessaloniki, 54124 Thessaloniki, Greece

HIGHLIGHTS

- The dominant control of SSD grains on the magnetic load of PG sands was revealed.
- Coarse, low-coercivity ferrimagnetic minerals were the dominant magnetic carriers.
- Fine SSD magnetic grains are the main carrier of anthropogenic metal(loid)s in PG sands.
- Metal(loid) contents were notably enriched in the magnetic fraction.
- Bioaccessible fractions ranging from 0.55% (Cr) to 48.22% (Cd) were estimated.

GRAPHICAL ABSTRACT

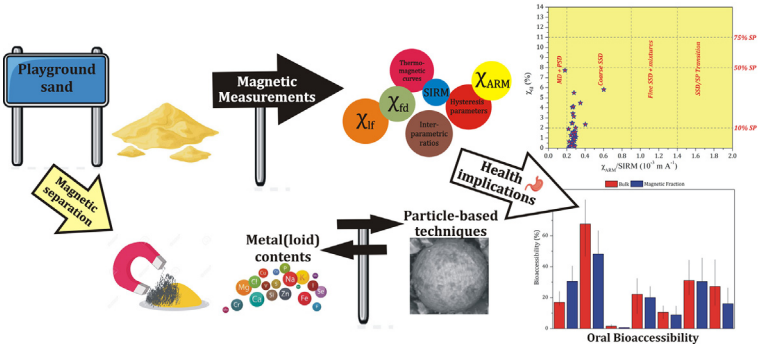

ARTICLE INFO

Article history:
Received 21 September 2021
Received in revised form 28 January 2022
Accepted 28 January 2022
Available online 2 February 2022

Editor: Filip M.G.Tack

Keywords:
Playground sand
Magnetic properties
Heavy metals
Bioaccessibility

ABSTRACT

Urban venues frequented by children, such as playgrounds, are potentially important sources of exposure to anthropogenic metal(loids). Environmental quality of outdoor playgrounds is mainly assessed through direct geochemical monitoring, which is time-consuming and expensive. In this study we adapted a multidisciplinary approach combining magnetic measurements, geochemical analyses, particle-based techniques and bioaccessibility data so as to evaluate the applicability of magnetic methods as a low-cost and easy-to-use technology to monitor pollution level in public playgrounds. Playground sands were collected and their magnetic characteristics were studied in detail aiming to gain helpful additional details in relation to the type, concentration and particle-size distribution of the sand-bound magnetic particles. The obtained χ_{lf} values indicated an enhanced level of sand-bound magnetic components, while the dominant control of SSD grains on the magnetic load of playground-PG sands was revealed. Hysteresis parameters and thermomagnetic curves indicated low-coercivity ferrimagnetic minerals, such as magnetite and/or maghemite, as the predominant magnetic carriers. Ratios of χ_{ARM}/χ_{lf} and χ_{ARM}/SIRM indicated the dominance of coarser anthropogenic magnetic grains in the sampled PG sands compared to other recreational areas. Correlation analysis among magnetic variables and reported metal(loid) contents designated χ_{ARM} as a more effective indicator for the detection of anthropogenic load in PG sand samples than χ_{lf} or SIRM. Simultaneously, through geochemical analyses in magnetic extracts separated from PG sands, metal(loid) contents were notably enriched in the magnetic fraction validating their strong affinity with sand-bound magnetic particles. Finally, bioaccessibility tests

* Corresponding author at: Chemical Process and Energy Resources Institute, Centre for Research and Tecnhology Hellas-CERTH, 6th km Charilaou-Thermi Rd, 57001 Thessaloniki, Greece.
E-mail address: annab@geo.auth.gr (A. Bourliva).

http://dx.doi.org/10.1016/j.scitotenv.2022.153600

revealed lower UBM-extracted fractions for the magnetic extracts of PG sands compared to bulk samples. However, arsenic (As) was more bioaccessible in the sand-bound magnetic particles raising serious concerns for the children exposed to playground sands.

1. Introduction

In urban agglomerations, substantial pollution levels can arise primary from traffic-related activities and enhanced fossil fuel combustion or even fossil fuel consumption for household activities. Non-biodegradable, accumulative metal(loid)s are the most broadly dispersed elements of concern, while their contents in various urban environmental media i.e. soils, sediments, road dusts, have become a critical issue for the health of the urban inhabitants (Bourliva et al., 2018; Adimalla et al., 2020; Liu et al., 2020; Shahab et al., 2020; Heidari et al., 2021; Ramazanova et al., 2021). Children, with less mature immune system, a still-developing respiratory tract and higher adsorption rates, are significantly more vulnerable to the harmful effects of metal(loid)s (Aleksander-Kwaterczak and Rajca, 2015) than adults. Thus, urban venues frequented by children, especially playgrounds, have attracted research interest as sites of exposure to anthropogenic metal(loids) that are distinctive and potentially significant (Ljung et al., 2006; Akinwunmi et al., 2017; Peng et al., 2019).

Outdoor playgrounds' environmental quality has received attention across the world and a substantial number of studies have been conducted in soils (Ljung et al., 2006; de Miguel et al., 2007; Acosta et al., 2009; Guney et al., 2010; Massas et al., 2010; Ademuyiwa et al., 2013; Reis et al., 2014; Sapcanin et al., 2017; Hiller et al., 2018, 2020; Rodriguez-Oroz et al., 2018; Rózański et al., 2018; Javed et al., 2019; Jin et al., 2019; Peng et al., 2019; Guo et al., 2020; Laha et al., 2020; Zgłobicki et al., 2020), dusts from pavements or equipment surface (Ng et al., 2003; Reis et al., 2014; Jin et al., 2019; Peng et al., 2019; Meza-Figueroa et al., 2020) and sands (Ottesen et al., 2008; Zgłobicki et al., 2020; Valido et al., 2018) focusing on the identification of highly impacted playground areas, apportionment of sources and pathways and evaluation of potential health risks. Moreover, in-vitro studies evaluated bioaccessible fractions of metal(loid)s with varied and often contradictory conclusions reflecting the abundant and composite parameters that determine bioaccessible loads in playground soil/dust or sand (Reis et al., 2014; Hiller et al., 2018; Valido et al., 2018; Laha et al., 2020). The vast majority of the conducted studies were based on direct geochemical monitoring, which is often time-consuming, labor-intensive and expensive. The last decades, magnetic approaches for monitoring environmental pollution are gaining popularity (Xie et al., 2001; Chan et al., 2001; Lecoanet et al., 2003; Kim et al., 2007) as a quick, easy, efficient, low-cost and non-destructive tool. Scientific reports on magnetic monitoring of playgrounds or playing fields, on the other hand, are sparse (Ng et al., 2003; Yang et al., 2017).

Magnetic monitoring is based on the fact that magnetic particles are effective absorbers and transporters of pollutants such as heavy metals or even organic contaminants due to their vast surface area (Halsall et al., 2008; Wang et al., 2012; Li et al., 2021). Thus, deposition and input of a significant amount of ferrimagnetic components, especially in urban agglomerations, result in a simultaneous enhancement of both magnetic signals and pollution loads. Many studies has ascertained the close relationship between magnetic properties and total elemental contents in most of which magnetic susceptibility is solely used because of its quick acquisition and good applicability as qualitative proxy for pollution in various environmental media (Wang et al., 2012; Xia et al., 2014; Aidona et al., 2016; Bourliva et al., 2017). However, there are cases in which poorer correlations between magnetic susceptibility and metal contents were reported, especially in small-scale assessment of contaminated sites (Schmidt et al., 2005), while several researchers report other concentration-dependent magnetic parameters such as saturation isothermal remanent magnetization-SIRM, and susceptibility of anysteretic remanent magnetization-χ_{ARM}, as more efficient indicators for the detection of anthropogenic loads (Xie et al., 2000; Shilton et al., 2005; Wang et al., 2013). Detailed magnetic characterization reflecting not only the concentration of magnetic particles for assessing pollution level, but also two specific features, their mineralogy and domain grain size, may provide proxies for identifying the possible natural and/or anthropogenic sources as well. Anthropogenic magnetic particles are relatively coarse grained within the multi domain (MD) range compared to the fine-grained superparametric (SP) and single domain (SD) particles of pedogenic origin (Magiera et al., 2007; Łukasik et al., 2014; Wang et al., 2017). Also, anthropogenic magnetic particles differ in terms of morphology and spherical-shaped magnetic particles may act as tracers of industrial dust deposition in the topsoils (Blaha et al., 2008; Xia et al., 2014). Additionally, ferromagnetic components, although being a fraction of the total amount of urban agglomerations, can be a health risk as they act as carriers of heavy metals. (Maher et al., 2016; Song et al., 2016). Kelepertzis et al. (2021) indicated magnetic measurements as a proxy for human health risks by revealing strong linkage among magnetic properties and bioaccessible amounts of metal(loid)s in urban soils and road dusts. All the above, reflect the necessity of multidisciplinary studies combining magnetic measurements, geochemical analyses, particle-based techniques (such as XRD analyses and SEM observations) and bioaccessibility data in order to draw clear conclusions.

Thessaloniki, the second largest city of Greece with over 1 million inhabitants in its metropolitan area, is not renowned for its parks and recreation areas as green spaces are few. Although, enough public playgrounds across the city have been renovated, there are still many outdated with no regular maintenance operations such as sand replacement, disinfection etc. by the public services, which raises concerns and necessitates monitoring. A recent study (Bourliva et al., 2021) has addressed the levels of potentially harmful elements (PHEs) in sands of public playgrounds where the anthropogenic loads were linked to magnetic components. All the same, limited relationships were established among magnetic susceptibility, metal contents and bioaccessibility data. In continuation, the aim of the present study was to determine the concentration of magnetic particles/grains, magnetic mineralogy and grain size as inferred from the domain state of magnetic particles originating from playground sands. The magnetic data were supplemented with geochemical analyses, particle-based techniques for mineralogical/morphological characterization and bioaccessibility data of the sand-bound magnetic particles aiming: (a) to explore magnetic properties as potential proxy for assessing pollution level in children-related venues; (b) to identify anthropogenic magnetic loads; and (c) to evaluate potential health implications to children exposed to sand-bound magnetic particles in public playgrounds.

2. Materials and methods

2.1. Study area and sampling

A total of 37 samples of playground sand (PG sand) were gathered from 34 public playgrounds throughout the city of Thessaloniki (N. Greece) as illustrated in Fig.S1 (Supplementary Material). Details on sampling sites and procedure are given in Bourliva et al. (2021). In brief, sands were sampled from the top layer (0–20 cm) at 3–7 spots on the playground, depending on the total surface area, trying to avoid as much as possible areas which are covered by treetops or at the playground's edge, as well as sites near flora or urban furniture. Sand samples were collected at the end of the dry season (August–September 2019). Unexposed sand samples i.e. clean sand not utilized before for other purposes (blank), were not available, so instead, a freshly replaced sand sample was gathered. Sand samples were placed in self sealed polyethylene bags and transported to the laboratory where they were homogenized, quartered, air-dried and mechanically sieved to provide the <500 μm and < 250 μm size fractions. For magnetic

measurements, approximately 10 g of each individual sample (<500 μm size fraction) was placed into a cubic plastic box (2 cm in size). Any contact with metallic materials throughout experimental procedures was avoided. The <250 μm size fraction was utilized for geochemical determinations and oral bioaccessibility tests in accordance to recommendations for young children's exposure assessments (Ruby et al. 1996). Even though magnetic properties are strongly dependent on the granulometric fraction, preliminary magnetic measurements in both size fractions (<500 μm and < 250 μm) indicated no statistically significant differences. Dytłow et al. (2019), indicated also no significant differences on determined concentration dependent magnetic variables among the 250-500 μm and 100-250 μm size fractions. For detailed characterization of sand-bound magnetic components, magnetic extracts from a sub-set of PG sand samples (<250 μm size fraction, increased χ_{lf} values) were obtained using a powerful neodymium magnet coated with a propylene bag, The extraction was carried out indefinitely until the magnet was free of magnetic particles. The magnetic fractions (MFs) that had been extracted, were collected and weighed.

2.2. Magnetic measurements

Anhysteretic remanent magnetization (ARM), with a steady direct current (DC) with bias field of 0.04 mT imparted in a peak alternating field (AF) of 100 mT, was induced by a Molspin-MSA2AF tumbler demagnetizer (Molspin, Newcastle, UK); then it was measured using a Molspin magnetometer and expressed as the susceptibility of ARM (χ_{ARM}). Isothermal remanent magnetization (IRM) was generated in a maximum "Saturation" field of 1000 mT ($SIRM_{1000mT}$), followed by a series of increasing reverse fields of −100 mT and − 300 mT (IRM_{-100mT}, IRM_{-300mT}) with a Pulse Magnetizer (ASC IM10–30) and measured using a Molspin magnetometer. A range of additional parameters were calculated to provide further information regarding magnetic grain size and mineralogy, including HIRM (HIRM = ($SIRM_{1000mT}$ + IRM_{-300mT})/2), HARD % (HARD = (HIRM/$SIRM_{1000mT}$)*100), S_{-100} (S_{-100} = IRM_{-100mT}/$SIRM_{1000mT}$), S_{-ratio} (S_{-ratio} = IRM_{-300mT}/$SIRM_{1000mT}$) and inter-parametric ratios χ_{ARM}/χ_{lf} and $\chi_{ARM}/SIRM_{1000mT}$. Magnetic hysteresis loops were recorded by a PAR 155 vibrating sample magnetometer (VSM) calibrated against a NIST certified Ni standard; all measurements were recorded at room temperature applying a maximum field of 2 T and magnetization (saturation magnetization-M_s and saturation remanence-M_{rs}) along with coercivity data (coercive force-B_c and coercivity of remanence-B_{cr}) were determined; paramagnetic contribution was removed by applying the law of approach to saturation. Thermomagnetic analyses, which assess the variations of low-field magnetic susceptibility (χ_{lf}) vs. temperature (T °C) were obtained by employing either a MS2 Bartington susceptibility meter with a MS2WF furnace attached (Paleomagnetic Lab, AUTH) for samples with high χ_{lf} values, or a MFK1 Kappabridge (Cams, Paleomagnetic Lab., Leoben University, Austria) for samples with low χ_{lf} values. Both experiments were realized in free air measuring the magnetic susceptibility constantly from room temperature to 700 °C and back. Curie temperatures were calculated with the method of inflection points using the second derivative method.

2.3. Analytical procedures

Mineralogical characterization of magnetic extracts of selected PG sand samples was carried out by means of X-Ray powder diffraction (XRPD) using a Philips PW1710 diffractometer (Eindhoven, The Netherlands). Ni-filtered copper Kα radiation was used energized to 35 kV and 25 mA. Randomly oriented samples were scanned continuously from 3° to 63° 2θ angles at a scanning speed of 1.2° min^{-1}. The intensity (counts) of individual reflections, the density, and the mass absorption coefficient (CuK_α) of the discovered mineral phases were used to semi-quantitatively characterize the mineral phases. Corrections were made using external standard mixtures of the main mineral phases present. The size and morphology of sand-bound magnetic particles were characterized using a scanning electron microscope (JEOL JSM-6390LV). A representative portion of the magnetic fraction of selected samples was sprinkled onto double-sided aluminum tape mounted on a SEM stub, carbon-coated and viewed through randomly selected fields of view. An X-ray energy dispersive spectrometer-EDX (INCA 300) was used to determine the magnetic particles' elemental composition. The elemental analyses were conducted in "spot mode", which involves focusing the beam on a particular spot within the range of view that is manually selected. Furthermore, polished thin sections of the magnetic fraction of selected sand samples were prepared and analyzed in order to study the internal morphology and structure of the magnetic particles.

Near-total elemental contents of magnetic extracts of a subset of PG sands were determined using inductively coupled plasma mass spectrometry (ICP-MS) after a multi acid ($HF-HNO_3-HClO_4-HCl$) digestion procedure at the accredited Acme Analytical Laboratories, Canada. The criteria for sand samples selection were the enhanced magnetic signal based on χ_{lf} values and elemental contents of bulk samples as determined in Bourliva et al. (2021). A statistical summary of total elemental contents of the bulk samples is provided in Table S2 (Supplementary Material). Quality Assurance and Quality Control (QA/QC) included reagent blanks, analytical duplicates and analyses of in house reference materials (multi-element soil standard OREAS25A-4A and OREAS45E). Results of the method blanks were always below detection limits. The recovery rates were estimated within ±10% of the certified value and analytical precision was better than ±5%.

In-vitro oral bioaccessibility tests were performed on the magnetic fractions of selected PG sand samples and compared to already determined bioaccessibility data of bulk PG sand samples. The oral bioaccessibility of metal(loids) was determined using the UBM (Unified BARGE Method) protocol, which has been validated against an in vivo model for As, Sb, Cd and Pb (Caboche, 2009; Denys et al., 2012) and simulates both the gastric (G-phase) and gastrointestinal (GI-phase) portions of the human digestive process. The analytical protocol is given in detail in the International Standard ISO 17924:2018 (ISO 17924, 2018). The bioaccessibility tests were carried out at the University of Aveiro's (Portugal) GeoBioTec Research Unit Laboratory. ICP-MS was used to determine the metal(loid)s extracted from UBM (in mg kg^{-1}).Blanks, duplicate samples and the UBM-specific certified reference material BGS102 (Hamilton et al., 2015) were used to validate the quality of the extraction processes. The bioaccessible fractions (*Baf %*), which indicate actual levels in the UBM-extracts and depend on the total elemental contents were computed as follows:

$$\mathrm{Raf}(\%) = \frac{C_{Bioaccessble}}{C_{Total}} \times 100$$

where $C_{Bioaccessible}$ and C_{Total} are the UBM-extracted concentrations (mg kg^{-1}) from either G or GI-phase and the total elemental concentrations (mg kg^{-1}), respectively, that were measured for each element in the magnetic fraction of PG sand.

2.4. Statistical analysis

Statistical analysis was performed with IBM SPSS Statistics package version 25.0 for Windows. All variables were checked for normality of their statistical distribution by the Shapiro-Wilk test. Interrelationships between magnetic and geochemical variables were evaluated by Pearson's correlation coefficient analysis, while interrelationships to pooled data from a sub-set of samples with enhanced magnetic signal were also screened. To identify significant differences across variables, analysis of variance (one-way ANOVA) was used.

3. Results and discussion

3.1. Magnetic properties of playground sands

3.1.1. Magnetic mineral content

The values of mass specific magnetic susceptibility (χ_{lf}) have been already discussed in a recent study by Bourliva et al. (2021, Table 1) where

Table 1
Descriptive statistics of the magnetic properties of playground sands in Thessaloniki, Greece.

Magnetic Parameters	Units	Mean	SD[a]	Median	Min	Max	CV[b]
χ_{lf}[c]	10^{-8} m^3 kg^{-1}	149.2	50.1	149.8	51.0	248.7	0.336
χ_{fd}[c]	%	1.29	1.80	1.30	0.11	7.73	0.937
χ_{ARM}	10^{-8} m^3 kg^{-1}	421.5	137.7	434.4	87.6	761.7	0.327
SIRM	10^{-5} Am^2 kg^{-1}	1534	500	1554.6	456.5	2306	0.326
S_{-100}	%	0.678	0.041	0.670	0.600	0.770	0.060
S_{-300} (S-ratio)	%	0.950	0.034	0.950	0.830	1.000	0.035
HIRM	10^{-6} Am^2 kg^{-1}	40.2	30.1	31.8	0.31	115.7	0.748
HARD	%	2.54	1.68	2.36	0.04	8.53	0.661
χ_{ARM}/SIRM	10^{-3} m A^{-1}	0.28	0.07	0.27	0.18	0.60	0.236
χ_{ARM}/χ_{lf}	Dimensionless	2.87	0.59	2.78	1.54	5.19	0.206
SIRM/χ_{lf}	kA m^{-1}	10.3	0.97	10.38	8.51	11.9	0.094
H_{cr}	mT	55.85	18.7	60.24	16.99	87.96	0.335
H_c	mT	17.68	6.29	17.50	8.5	34	0.356
M_s	Am^2 kg^{-1}	0.153	0.049	0.149	0.074	0.301	0.323
M_r	Am^2 kg^{-1}	0.015	0.007	0.014	0.005	0.037	0.512

[a] SD: standard deviation.
[b] CV: coefficient of variation.
[c] Summary statistics of χ_{lf} and χ_{fd} values are from Bourliva et al., 2021.

a range of 51–248.7 × 10^{-8} m^3 kg^{-1} (with a median of 149.8 × 10^{-8} m^3 kg^{-1}) was reported indicating an enhanced level of anthropogenic sand-bound magnetic components in the PG sands. Despite the limited data, the obtained χ_{lf} values were within the ranges reported by other researchers (Table S1, Supplementary Material) for playground dusts (Ng et al., 2003; Yang et al., 2017), while they are notably higher than the χ_{lf} values referred for urban park soils (Lu and Bai, 2006; Wang et al., 2017) and street dusts (Dytłow et al., 2019). In addition, SIRM and χ_{ARM}, which are characteristic concentration related magnetic parameters, were evaluated. SIRM represents the entire amount of remanence-bearing material, even though it is often dominated by ferrimagnetic material. SIRM ranged between 456.5 ×10^{-5} Am^2 kg^{-1} to 2306 ×10^{-5} Am^2 kg^{-1} with a median value of 1554.6×10^{-5} Am^2 kg^{-1}. A strong positive linear correlation (Adj. R-Square = 0.936) among χ_{lf} and SIRM was evident (Fig. 1a) underscoring the dominance of ferrimagnetic minerals to the magnetic signal of the PG sands. On the other hand, χ_{ARM}, which is sensitive to stable single-domain (SSD) grains (Maher, 1988; Heider et al., 1996), exhibited a range of 87.6–761.7 ×10^{-8} m^3 kg^{-1} with a median value of 434.4×10^{-8} m^3 kg^{-1}, while the significant correlation with the χ_{lf} values (Fig. 1a, Adj. R-Square = 0.657) revealed the dominant control of SSD grains on the magnetic load of PG sands. This is also portrayed by the significantly higher χ_{ARM} values compared to previous studies (Table S1, Supplementary Material) in soils and dusts in urban agglomerations (Xia et al., 2014; Wang et al., 2014; Zhao et al., 2020; Dytłow et al., 2019; Shilton et al., 2005), despite the lack of reported data for urban playing or recreation areas.

3.1.2. Magnetic mineralogy

The S-ratio provide an index of relative contributions to SIRM of high- / low-coercivity materials. Values close to unity imply a substantial contribution of low-coercivity (ferrimagnetic) magnetic minerals, such as magnetite and/or maghemite, whereas lower values suggest the predominance of more high-coercivity magnetic (antiferrimagnetic) minerals (Bloemendal et al., 1992). The S-ratio values of the studied PG sands varied from 0.830 to 1.000 with an average of 0.950 (Table 1) indicating that soft, low-coercivity magnetite-type ferrimagnetic minerals were the predominant magnetic carriers in the PG sands. Only two samples (PG4 and PG17) indicated S-ratio values <0.90. The complete total content of high-coercivity magnetic minerals, such as hematite and goethite, is described by HIRM

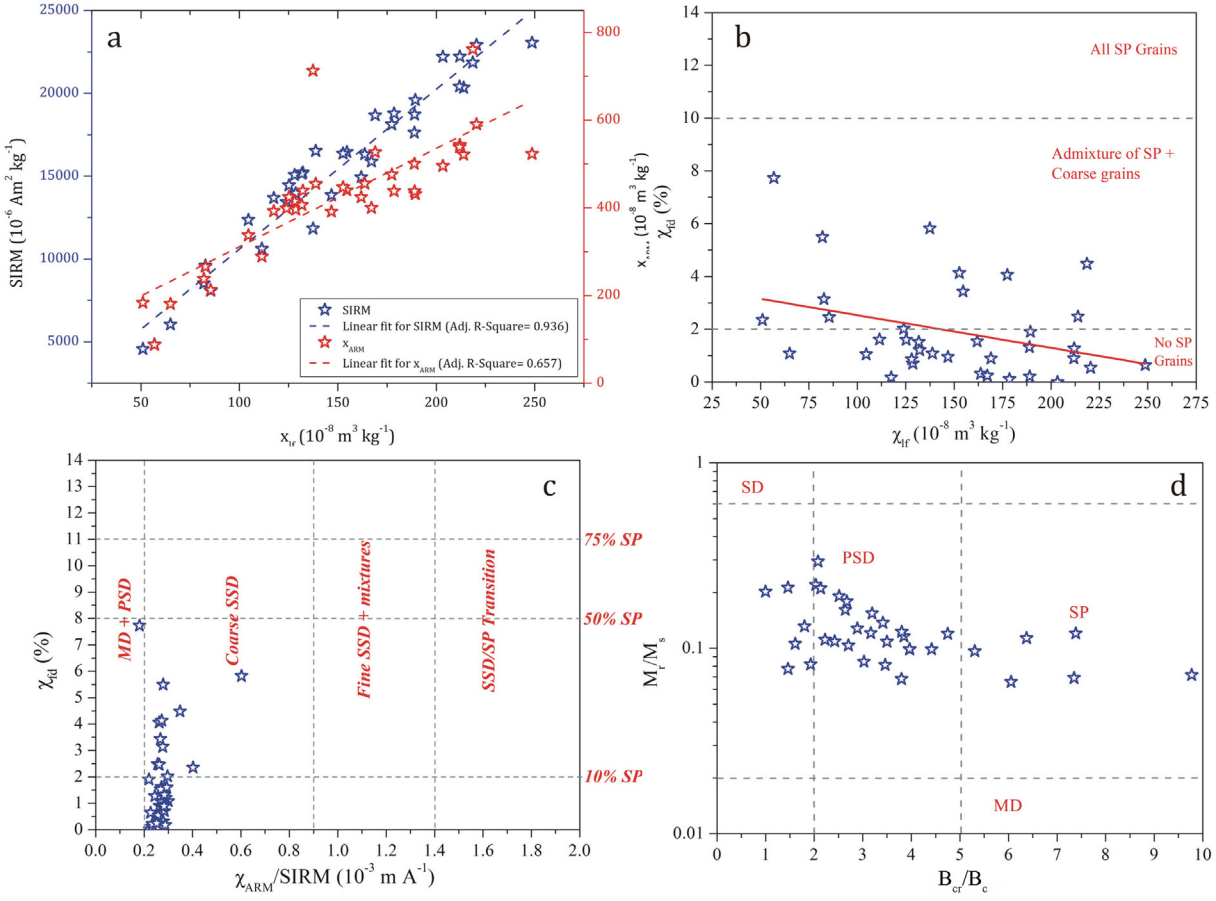

Fig. 1. Scatter plots of a) SIRM and χ_{ARM} versus χ_{lf}, b) χ_{fd} % versus χ_{lf}, c) χ_{fd} % versus the ratio χ_{ARM}/SIRM (cf. the "Dearing plot" (Dearing et al., 1996)) and d) Day plot of M_r/M_s versus H_{rc}/H_c of playground sands from Thessaloniki, Greece.

(Thompson and Oldfield, 1986). The HIRM ranged from 0.31 to 115.7 × 10^{-5} Am^2 kg^{-1} with a mean value of 40.2 × 10^{-5} Am^2 kg^{-1} (Table 1). The HARD% ranged from 0.04 to 8.53% with an average of 2.54% verifying that high-coercivity minerals in the PG sands have a negligible contribution to magnetization. However, the same two samples (PG4 and PG17) showing high HIRM and HARD% values coupled with low S-ratio values ascertained the relatively higher hematite/goethite contents. Magnetic mineralogy was also confirmed through hysteresis loops (Fig. 2a-c) and temperature dependent susceptibility (χ-T) curves (Fig. 2d-f). The hysteresis loops were in most cases "narrow-shaped", presenting low values of remanence and coercivity; specific magnetization reached the 90% of its saturation value at relatively low external magnetic field at about 300 mT clearly indicating the dominance of low-coercivity ferrimagnetic minerals in playground sand samples (Liu et al., 2019). Thermomagnetic curves (χ-T) for the majority of PG sands (Fig. 2d-f) indicate a similar trend during heating with a significant decrease of susceptibility at a range of 560–580 °C, identifying a magnetite-like phase as the predominant magnetic carrier. However, there is a limited number of sand samples where slightly higher Tc values (around 600 °C) were observed (Fig.2d) suggesting a probable maghemitization (formation of maghemite (T_c = 640 °C) shells) of the magnetite grains (Szuszkiewicz et al., 2015). The presence of maghemite in PG sands was also verified by a slight increase of susceptibility at 280–300 °C (Li et al., 2014; Wang et al., 2014, Wang et al., 2019a, b; Zhao et al., 2020). This minor peak in the heating curve (especially in cases where no simultaneous increased T_c values was observed) could be also attributed to the presence of trace amounts of sulphides (Zheng and Zhang, 2008; Magiera et al., 2011). In addition, the relative smooth decrease in magnetic susceptibility between 500 and 580 °C, recorded in some PG sand samples, may suggest the presence of a mixture of magnetite and maghemite or a wide grain-size distribution of magnetite (Magiera et al., 2011). Other effects in the heating curves related to the presence of divert grain sizes of magnetite (Dunlop, 2014; Szuszkiewicz et al., 2015), were also recorded in many cases, such as a slight decrease in susceptibility at around 400 °C and/or a subsequent gradual increase of susceptibility around 450–500 °C, known as Hopkinson peak. The Hopkinson effect was observed more pronounced in more anthropogenically impacted sand samples (Bourliva et al., 2021) in agreement with prior research (Aguilar-Reyes et al., 2011; Jeleńska et al., 2004). In all cases, the cooling curves were above the heating curves (Fig.2d-f), showing enhanced susceptibility after completion of the χ-T runs, indicating the formation of strongly magnetic phases during heating procedure (Zhu et al., 2012; Li et al., 2014; Szuszkiewicz et al., 2015).

3.1.3. Grain size of magnetic minerals

Frequency-dependent magnetic susceptibility (χ_{fd}%) is widely used to reflect the amount of ultrafine superparamagnetic (SP) grains (Dearing et al., 1996). Our recent study (Bourliva et al., 2021) exhibited values of χ_{fd}% below 4% (median 1.29%) implying a negligible amount of ultrafine superparamagnetic (SP) grains in most of the studied sand samples (Dearing et al., 1996). A weak but significant negative correlation between χ_{lf} and χ_{fd} % (Fig1b, Pearson's $r = -0.344$, $p < 0.05$) further indicates a decrease of SP grains with magnetic enhancement of PG sands. The interparametric ratios χ_{ARM}/χ_{lf} and χ_{ARM}/SIRM are also often applied as grain size indicators where higher values indicate finer particles. The values of χ_{ARM}/χ_{lf} for PG sands ranged from 1.54 to 5.19 (mean 2.87) suggesting the presence of different grain sizes of magnetic grains in PG sands (Table 1). Even though a comparison of magnetic parameter values among divergent places and areas of interest would be quite difficult due to differences in magnetic particle sources and geochemical background, the values obtained were much higher than those reported by several researchers (Table S1. Supplementary Material) for topsoils (Xia et al., 2014; Wang et al., 2014) and road dusts (Zhao et al., 2020; Wang et al., 2019a, 2019b; Yang et al., 2021) in multiple urban agglomerations suggesting the contribution of relatively finer magnetic particles. Nevertheless, the obtained mean χ_{ARM}/χ_{lf} values were lower than those of soils in urban parks (3.1–3.9) in Shanghai, China (Wang et al., 2017) indicating the dominance of coarser anthropogenic magnetic grains in the sampled PG sands compared to other recreational areas. Similarly, the mean value of χ_{ARM}/SIRM (0.28 × 10^{-3} m A^{-1}) was significantly higher than those reported in previous studies (Table S1, Supplementary Material) for urban

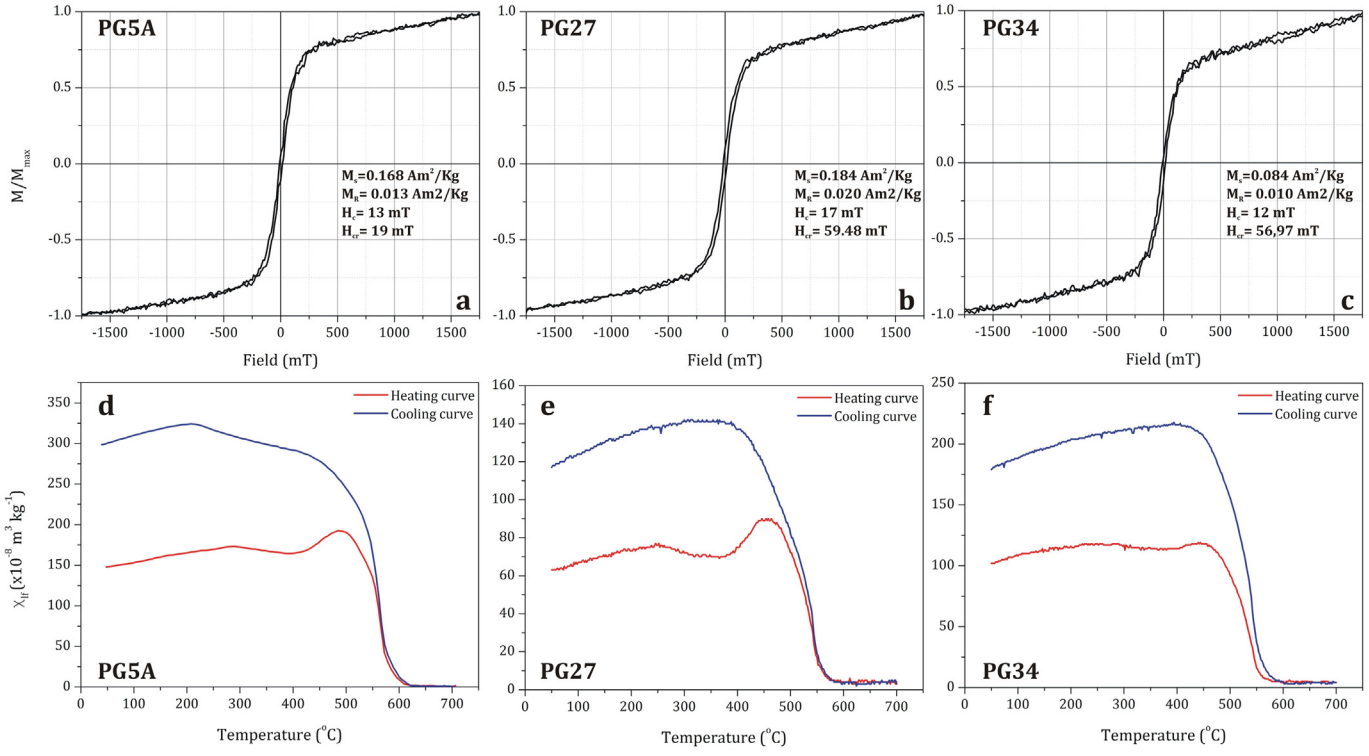

Fig. 2. Magnetic hysteresis loops with maximum filed of 2.0 T (a-c) and thermomagnetic curves (d-e) of representative playground sand samples from Thessaloniki, Greece. M_s parameter estimation does not include paramagnetic contribution.

environmental media (Xia et al., 2014; Wang et al., 2014; Zhao et al., 2020; Wang et al., 2019a, 2019b; Xie et al., 1999; Yang et al., 2021) indicating finer magnetic grains in the PG sands, while they were within the ranges reported by Wang et al. (2017) for soils of urban parks in Shanghai, China. The size of magnetic grains can also be depicted by the scatter plot of χ_{fd} % versus χ_{ARM}/SIRM (Fig.1c), based on Dearing et al. (1996), where the majority of PG sands lied in the bottom left of the region of coarse SSD suggesting coarse grained ferrimagnetic minerals. To evaluate the grain size of magnetic particles in more detail, Day plot (Dunlop, 2002) was employed based on the ratios of the hysteresis parameters (B_{cr}/B_c and M_r/M_s) (Fig. 1d). Most sand samples plot in the PSD area, while some distinct samples plot in the MD interval indicating coarse grains in line with previous studies (Aidona et al., 2016).

3.2. Characterization of magnetic fraction of playground sands

To further characterize the magnetic particles of PG sands and provide detailed information regarding the grain sizes and forms of sand-bound magnetic particles XRD analysis and SEM observations were applied. Mineralogy of bulk PG sands indicated siliceous or feldspathic sands, while limited samples exhibited high halite contents suggesting a coastal or marine source (Bourliva et al., 2021). On the other hand, the so called "heavy minerals", which are of natural origin and are a common feature of sands (Wills and Finch, 2016), mainly include magnetite and/or maghemite, hematite and minerals containing Ti such as anatase, rutile, ilmenite. In our case, magnetic extracts of selected PG sand samples were mineralogically characterized. A Fe-spinel phase with a distinct peak at around 35.5° 2-theta (~2.52 Å) was recorded (Fig. 3), which lies between that of magnetite (Fe_3O_4) and maghemite (γ-Fe_2O_3), indicating a probable mixture of both phases in line with the magnetic mineralogy data. Besides, the identification between magnetite and maghemite is rather difficult due to their overlapping diffraction peaks (Kim et al., 2012). On the other hand, non-magnetic crystalline phases such as quartz, plagioclase, calcite, sheet-silicates, mainly micas and chlorite, and amphiboles were also detected due to the presence of aggregates of magnetic and non-magnetic particles. Moreover, amorphous material observed as a hump between 10-20° 2-theta in the diffraction patterns can be attributed to non-crystalline phases or the absorption of the plastic sampler holder.

Furthermore, SEM observations on separated magnetic fractions were performed. Magnetic extracts were dominated by Fe-rich irregular agglomerates and subhedral to anhedral crystalline grains (Fig. 4) with subordinate amounts of Al, Si, Cr, Mn, and Ti. Numerous anthropogenic magnetic spherical particles were detected (Fig.4a-d) indicating the impact of adjacent anthropogenic activities in PG sands. Iron-rich spherules are characteristic in the magnetic fractions of urban environmental media as previously supported by several researchers (Ault et al., 2012; Bourliva et al., 2016; Kelepertzis et al., 2019, 2021) exhibiting variable particle sizes and diameters (from 1 to 100 μm). Ferrospheres with diverse surface structures such as polygonic-pattern (Fig. 4a-b) and orange-peel (Fig.4c) were identified in the PG sands, while spherical particles with noticeable holes ("cenospheres") (Fig. 4d) or hollow spherical particles filled with finer spherules or other magnetic particles ("plerospheres") were also detected. EDX analysis indicated an iron content of >85% for the examined magnetic spherules with elements Al and Si being present in most of the cases, while Mg, Mn and Ti were only detected in specific particles. A further study performed on the inner structure of magnetic particles on thin polished sections, revealed spherical particles with interior holes (Fig.4e-f) and others with holes that encapsulated sub-microspheres or magnetic particles of different size (Fig.4g-h) with a high Fe content reaching up to 98% in some cases.

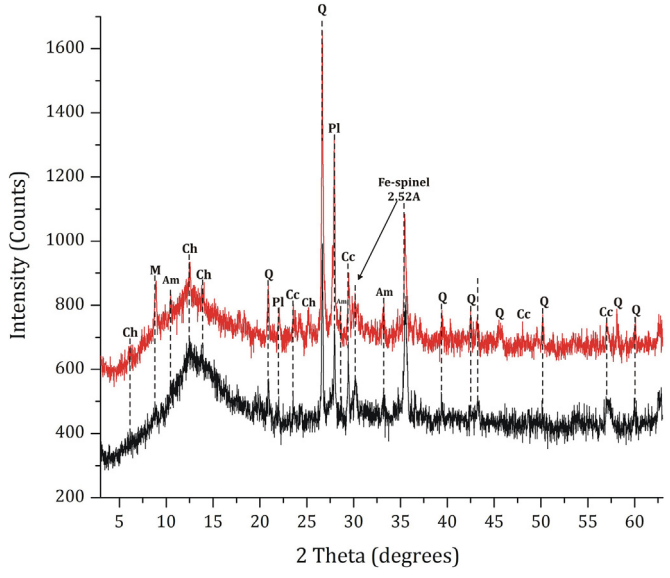

Fig. 3. Representative XRD patterns of magnetic extracts from selected playground sands. The most intense reflections of respective minerals are labeled. Fe-Spinel: iron spinel phase, Ch: Chlorite, M: Micas, Am: Amphiboles, Q: quartz, Pl: Plagioclase, Cc: calcite.

3.3. Linkage of magnetic properties with elemental contents

To investigate whether magnetic parameters can be utilized as proxies for the contamination degree on the studied playgrounds, the correlation between magnetic parameters and elemental contents (bulk samples) of the PG sands was examined (Table 2). The total elemental contents of the bulk PG sands were discussed in a previous study (Bourliva et al., 2021), however a statistic summary of the determined concentrations for both major and trace elements is provided in Table S2 (Supplementary Material). No significant correlations were revealed between the concentrations of the elements tested in this study and χ_{lf} or SIRM (Table 2) in contrast to reports of other researchers in various urban environmental media (Lu and Bai, 2006; Li et al., 2014; Wang et al., 2019b). The only exception was Cr which exhibited a significant ($p < 0.05$) positive correlation with both χ_{lf} (0.382) and SIRM (0.357). Better correlations were revealed among Bi (0.337), Ni (0.451) and Sn (0.449) contents and χ_{ARM} (Table 2) suggesting their association with finer, mainly SSD, magnetic particles probably from distant sources (Hu et al., 2007) and designating χ_{ARM} as a more effective indicator for anthropogenic load detection in PG sand samples than χ_{lf}. Furthermore, positive significant ($p < 0.01$) correlations were revealed between grain size inter-parametric ratios χ_{ARM}/χ_{lf} and χ_{ARM}/SIRM with As (0.526 and 0.573, respectively), Cu (0.589 and 0.574, respectively), Ni (0.690 and 0.793, respectively) and Sn (0.436 and 0.469, respectively) indicating that finer magnetic particles are accompanied by relatively higher elemental contents (Table 2). This finding contradicts previous studies where strong negative correlations are reported between χ_{ARM}/SIRM and heavy metal contents indicating their association with coarser magnetic grains in urban environments (Wang, 2013; Li et al., 2014). This fact comes to enforce our speculations that the probable origins of sand-bound magnetic particles in the studied playgrounds are from distant sources.

The weak correlations among magnetic parameters and elemental contents, in general, could be probably explained by the high content of geogenic material in the PG sands. Moreover, the inclusion of "non-polluted" PG sands with low magnetic load into the statistical analysis can affect the obtained results as previously reported by several researchers (Beckwith et al., 1996; Schmidt et al., 2005). Therefore, Pearson's correlation analysis was also applied on pooled data from a sub-set of sand samples ($n = 12$) with elevated χ_{lf} values (>175 × 10^{-8} m^3 kg^{-1}). In the most "impacted" PG sand samples correlations among Pb and Zn contents and both concentrations related magnetic parameters χ_{lf} and SIRM (Table 2) were revealed. Moreover, a statistically significant correlation was revealed between the concentration related magnetic variables, χ_{lf} and SIRM, and integrated pollution load index (PLI) (Bourliva et al., 2021) suggesting their efficient proxy indicator of the total anthropogenic load into high impacted playing areas (data not shown). In addition, the obtained correlation

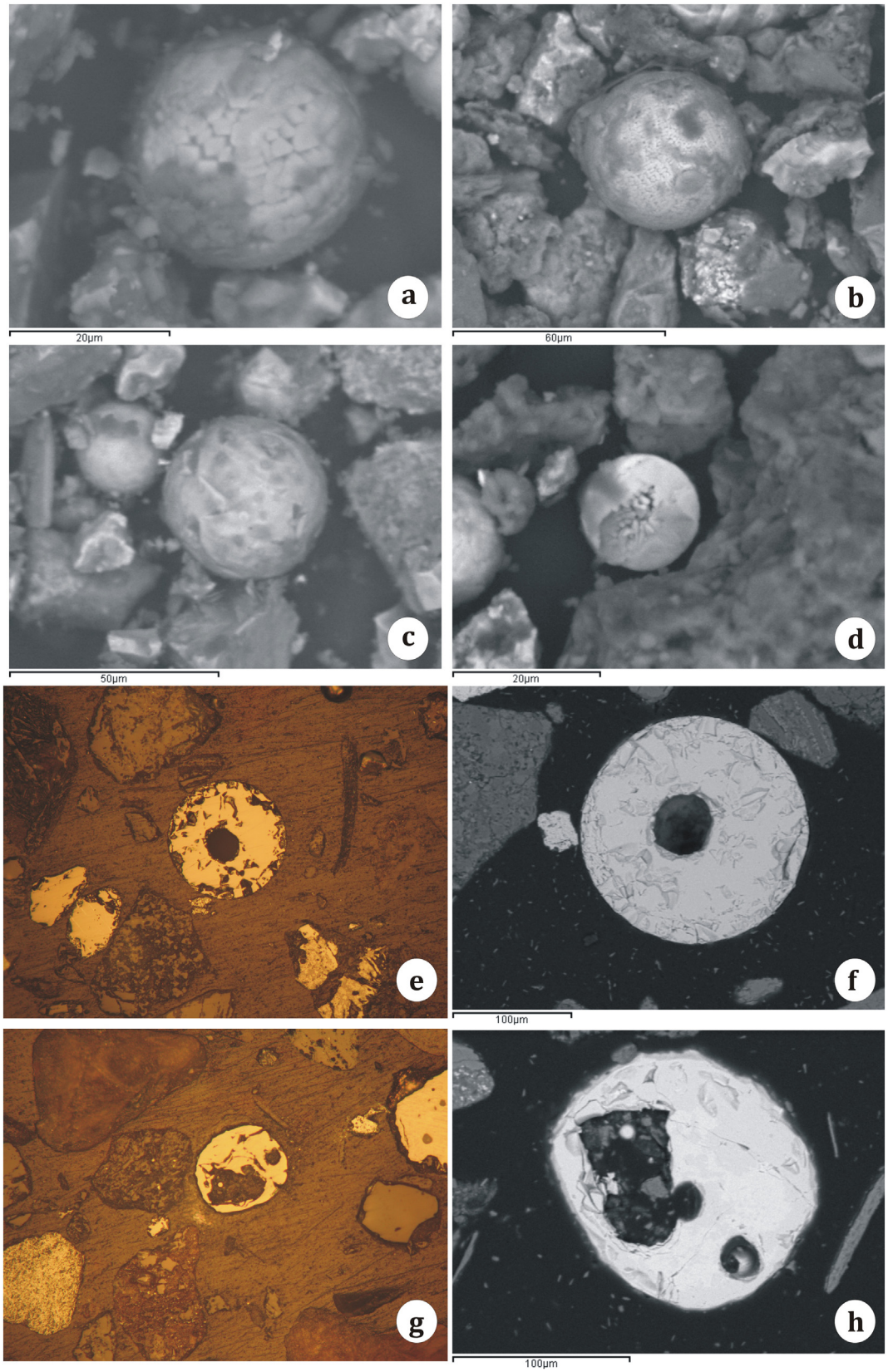

Fig. 4. Images of spherical magnetic particles detected in magnetic extracts separated from playground sands particles. a-b) SEM images of "polygonic" Fe-rich spherules; c) SEM image of an "orange peel" Fe-rich spherule; d) SEM images of an Fe-rich "plerosphere"; e-f) optical microscopy images of magnetic particles with internal holes from thin polished sections of magnetic extracts and; g-h) SEM images of the same magnetic particles with internal holes from thin polished sections of magnetic extracts.

Table 2
Pearson correlation coefficients among magnetic parameters and metal(loid) contents for playground sands in Thessaloniki, Greece. Bold ($p < 0.01$) and underlined ($p < 0.05$).

		As	Bi	Cd	Cr	Cu	Fe	Ni	Pb	Sn	Zn	PLI
Total dataset of PG sands ($n = 37$)	χ_{lf}	−0.387	0.123	0.061	0.382	−0.235	0.276	0.063	0.036	0.135	−0.199	−0.049
	$\chi_{fd\%}$	0.253	0.162	−0.109	−0.113	0.183	−0.129	0.232	−0.213	0.175	0.020	−0.048
	χ_{ARM}	−0.100	0.337	0.012	0.202	0.095	0.245	**0.451**	0.056	**0.449**	−0.101	0.021
	SIRM	−0.408	0.108	0.068	0.357	−0.229	0.226	0.002	0.069	0.121	−0.174	−0.032
	S-ratio	−0.016	−0.024	0.114	−0.051	−0.192	−0.141	**−0.480**	−0.012	−0.115	0.106	−0.166
	SIRM/χ_{lf}	−0.105	−0.099	0.079	0.045	0.029	−0.188	−0.177	0.170	−0.066	0.049	0.088
	χ_{ARM}/χ_{lf}	**0.526**	0.243	−0.062	−0.190	**0.589**	0.036	**0.690**	0.090	**0.436**	0.159	0.210
	χ_{ARM}/SIRM	**0.573**	0.277	−0.102	−0.199	**0.574**	0.134	**0.793**	0.007	**0.469**	0.127	0.189
Subset of PG sands $\chi_{lf} > 175 \times 10^{-8}$ m^3 Kg^{-1} (n = 12)	χ_{lf}	−0.066	0.148	0.189	0.165	0.103	0.410	−0.292	**0.546**	−0.086	0.308	**0.792**
	$\chi_{fd\%}$	**0.883**	0,751	−0.390	−0.179	0.474	0.056	0.247	0.642	**0.934**	**0.815**	0.087
	χ_{ARM}	0.705	**0.832**	0.050	−0.220	0.619	0.155	0.155	0.699	0.655	**0.785**	0.226
	SIRM	−0.009	0.232	0.237	−0.108	0.040	0.279	−0.526	**0.523**	−0.072	0.409	**0.782**
	S-ratio	0.331	0.043	−0.586	0.085	0.245	0.058	0.587	−0.192	0.328	−0.041	−0.357
	SIRM/χ_{lf}	0.061	0.132	0.134	−0.431	−0.104	−0.161	−0.425	0.009	0.005	0.178	0.061
	χ_{ARM}/χ_{lf}	**0.833**	**0.862**	−0.010	−0.334	0.650	−0.037	0.361	0.501	**0.778**	0.713	−0.163
	χ_{ARM}/SIRM	**0.790**	**0.791**	−0.062	−0.172	0.670	0.010	0.514	0.466	0.753	0.620	−0.199

χ_{lf}: mass-specific magnetic susceptibility; χ_{fd}: frequency dependent susceptibility; χ_{ARM}: susceptibility of anhysteretic remanent magnetization; SIRM: Saturation isothermal remanent magnetization; S-ratio: $= IRM_{-300mT}/SIRM_{1000mT}$.

coefficients among elemental contents and χ_{ARM} (Table 2) were significantly improved for Bi (0.832) and Sn (0.655), while strong associations were also observed for other anthropogenic related elements such as As (0.705), Pb (0.699) and Zn (0.785) underscoring χ_{ARM} as an even more efficient indicator in highly impacted playground environments and finer SSD magnetic particles as the primary carrier of potentially harmful trace elements in PG sands. Moreover, significant correlations were revealed among As (0.883), Bi (0.751), Pb (0.642), Sn (0.934) and Zn (0.815) and χ_{fd} % where in combination with the low (<2%) χ_{fd} % values in this subset of samples supplements our previous findings indicating probable anthropogenic sources. Similarly, the higher correlations among grain size inter-parametric ratios χ_{ARM}/χ_{lf} and χ_{ARM}/SIRM and elemental contents of As, Cu, and Bi in the PG sands along with the significant correlations revealed with Bi, Pb and Zn validated the association of sand-bound anthropogenic elements with finer magnetic grains.

To further enforce the linkage of the determined elemental contents with sand-bound magnetic particles, the geochemical properties of the MFs of selected PG sands were investigated. Iron (Fe) was enriched, as expected, in the magnetic fractions exhibiting a range of 8.98–13.9% compared to a range of 2.55–3.44% in the bulk PG sand samples further implying ferromagnetic particles as the primary magnetic carriers (Table S2, Fig. 5a). Moreover, Ti revealed significantly higher contents in the MFs of PG sands, as already verified from SEM observations, with an average of 0.531% compared to 0.165% in the bulk PG sands. Regarding trace elements, most of the studied elements (except As, Bi and Sn) exhibited significantly (one-way ANOVA, $p < 0.01$) higher concentrations compared to bulk sand samples (Table S2, Fig. 5a). Based on mean values a descending order of Mn > Cr > Ba > Zn > V > Ni > Pb > Co > Cu > As > Sn > Cd > Bi (Table S2, Supplementary Material) was observed, while Cr and V recorded the highest enrichment ratios i.e. ratio of element concentration in the magnetic and bulk fraction (Fig.5b). Thus, Cr recorded significantly higher concentrations ranging between 601 mg kg^{-1} and 1280 mg kg^{-1} in the MFs compared to those in the bulk PG sands that ranged between 102 mg kg^{-1} and 269 mg kg^{-1} (Table S2, Supplementary Material). Anthropogenic elements such as Zn, Pb, and Cu, were also relatively enriched in MFs of PG sands (mean enrichment ratios 2.0–2.9) with average contents of 201 mg kg^{-1}, 63.7 mg kg^{-1} and 36.8 mg kg^{-1} compared to the recorded ones in bulk samples of 72.4 mg kg^{-1}, 32.1 mg kg^{-1} and 16.4 mg kg^{-1}, respectively, indicating sand-bound magnetic particles as the probable main carriers of potentially harmful trace elements. Similar strong enhancements in the elemental contents of magnetic fractions separated from road dusts sampled in the city of Thessaloniki were found in a previous study in the broader area (Bourliva et al., 2016), which led us to suspect a possible supplemental traffic-related input for the sand-bound magnetic particles in the studied playgrounds.

3.4. Health implications of magnetic fractions of playground sands

The potential health consequences to children exposed to sand-bound magnetic particles in public playgrounds were assessed through oral bioaccessibility tests and the bioaccessible concentrations (mg kg^{-1}) are

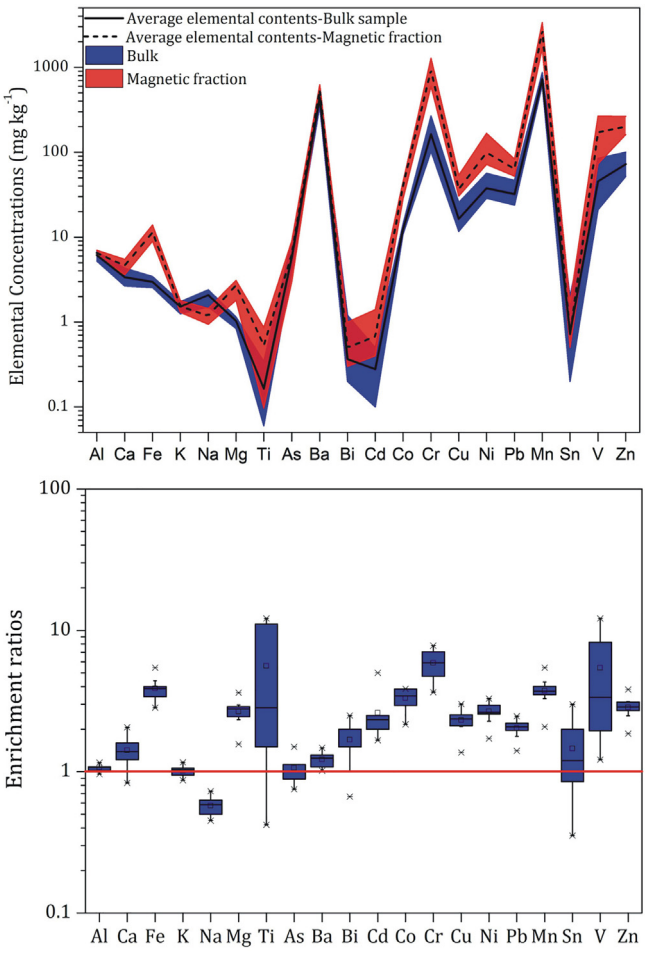

Fig. 5. a) Obtained ranges and mean values of concentrations of major (in %) and trace (in mg kg^{-1}) elements in the bulk and magnetic fraction of playground sands and; b) enrichment ratios of major and trace elements of playground sands from Thessaloniki, Greece.

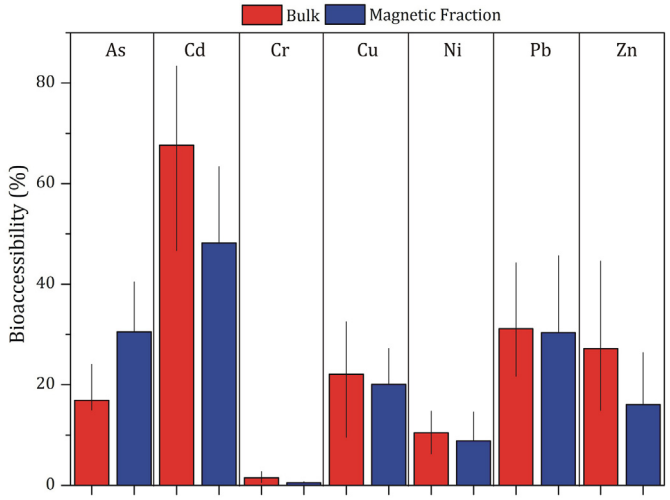

Fig. 6. Bioaccessible fractions (%) in the bulk and magnetic fraction of playground sands from Thessaloniki, Greece. Only values for the gastric phase (G-phase) are given. Bioaccessibility data for bulk playground sands are from Bourliva et al. (2021) and are given only for comparison reasons.

presented in Table S3 (Supplementary Material), while the relative bioaccessible fractions (BAF%) of selected trace elements are illustrated in Fig. 6. Only the results from the gastric phase will further be taken into account in this study as they offer the highest values from the bioaccessible compartments and are also thought to allow a more conservative risk assessment (Farmer et al., 2011). Moreover, bioaccessibility data regarding the bulk PG sands (Bourliva et al., 2021) are given for comparison reasons.

The mean UBM-extractable concentrations were 1.58 mg kg^{-1} for As, 0.37 mg kg^{-1} for Cd, 4.54 mg kg^{-1} for Cr, 6.76 mg kg^{-1} for Cu, 7.21 mg kg^{-1} for Ni, 20.55 mg kg^{-1} for Pb and 29.98 mg kg^{-1} for Zn, respectively, being notably higher than those recorded for the bulk PG sands (Table S2, Supplementary Material). However, bioaccessible fractions (Baf%) indicated a different trend with mean values decreasing in the order Cd (48.22%) > As (30.54%) > Pb (30.36%) > Cu (20.09%) > Zn (16.08%) > Ni (8.86%) > Cr (0.55%). The UBM-extractable fractions of metal(loid)s in the sand-bound magnetic particles are, in contrast, systematic lower than those reported for bulk PG sands (Fig.6), however Cd and Pb still displayed high bioaccessibility fractions, indicating that a significant portion of these anthropogenic metals is readily bioavailable through ingestion. A substantial difference was noticed for arsenic where higher bioaccessibility rates were observed compared to bulk PG sands. Specifically, the values of Baf % in the MFs ranged from 24.58 to 40.43% (mean 30.54%), while it ranged from 15.76 to 24.06% (mean 18.59%) in the bulk PG sands. Thus, arsenic, which is a highly toxic metalloid, was presented more bioaccessible in the magnetic fractions of PG sands suggesting the presence of As phases in the sand-bound magnetic particles that are highly soluble in the UBM-simulated gastric solution. Furthermore, the strong correlation (0.763, $p < 0.01$) revealed among As bioaccessible fractions and Fe_{tot} (<250 μm) validated the linkage of As readily bioaccessible phases with iron-bearing soluble phases. Besides, numerous studies have identified Fe oxyhydroxides as important factors determining As bioaccessibility where As is naturally abundant in soil (Wragg et al., 2007; Appleton et al., 2012; Kim et al., 2014; Palumbo-Roe et al., 2015).

Metal(loid)s such as Cd, As or Pb, even at low concentrations, can be acutely or severely harmful to human health due to their persistent nature and severe bio-accumulation and bio-magnification in the body tissues. Therefore, excessive bioaccessible amounts of such metal(loid)s in playground sands that could penetrate the body tissues through ingestion would endanger children's health and pose serious health hazards, such as lowered intellect, damage to the central nervous and immunological systems, and effects on internal organs, among other things. Thus, despite the fact that the sand-bound magnetic particles are no more than a fraction of the bulk samples, the enhanced bioaccessiblity rates raise serious concerns for children exposed to playground sands and render essential epidemiological studies in order to reach clear and accurate conclusions.

4. Conclusions

This study adapted a multidisciplinary approach combining magnetic measurements, geochemical analyses, particle-based techniques (including XRD analyses and SEM observations) and bioaccessibility data in order to evaluate the applicability of magnetic methods as a simple and low-cost tool for monitoring pollution level in public playgrounds. The obtained χ_{lf} values ranging between 51 and 248.7×10^{-8} m^3 kg^{-1} indicated an enhanced level of sand-bound magnetic components, while a significant correlation among χ_{ARM} and χ_{lf} revealed the dominant control of SSD grains in PG sands. Hysteresis parameters and thermomagnetic curves indicated soft, low-coercivity ferrimagnetic minerals, such as magnetite and/or maghemite, as the predominant magnetic carriers. Combined with SEM observations, numerous characteristic Fe-rich spherules with various structures were found indicating an anthropogenic input. In advance, the ratios of χ_{ARM}/χ_{lf} and χ_{ARM}/SIRM indicated the dominance of coarser anthropogenic magnetic grains in the sampled PG sands compared to other recreational areas and in accordance to "Dearing plot" revealed the dominance of coarse SSD magnetic grains. Incorporation of geochemical data into magnetic determinations designated χ_{ARM} as a more efficient indicator for the detection of anthropogenic load in PG sand samples. In addition, geochemical analyses in magnetic extracts indicated notably enhanced metal(loid) contents validating their strong affinity with sand-bound magnetic particles and rendering magnetic techniques as an efficient tool for monitoring pollution level in highly impacted playgrounds. Finally, for the first time, bioaccessibility tests performed on magnetic extracts from PG sands revealed risk-elements such as Cd, As and Pb which exhibited bioaccessibilities >30% indicating that a significant fraction of these anthropogenic metals is readily bioavailable through sand ingestion by children exposed to public playgrounds. Specifically, arsenic (As), a highly poisonous metalloid, was shown to be more bioaccessible in the sand-bound magnetic particles compared to bulk samples, presenting severe concerns and necessitating further epidemiological and toxicological research in order to draw clear and precise conclusions.

CRediT authorship contribution statement

Anna Bourliva: Conceptualization, Investigation, Data curation, Validation, Resources, Visualization, Writing – original draft, Writing – review & editing, Funding acquisition. **Eleni Aidona**: Conceptualization, Investigation, Validation, Resources, Writing – review & editing, Supervision; **Lambrini Papadopoulou**: Investigation, Formal analysis, Writing – review & editing; **Eduardo Ferreira da Silva**: Formal analysis, Validation, Resources, Writing – review & editing; **Carla Patinha:** Methodology, Formal analysis, Validation, Resources, Writing – review & editing; **Charalambos Sarafidis**: Methodology, Investigation, Formal analysis, Writing – review & editing; **Nikolaos Kantiranis**: Investigation, Formal analysis, Writing – review & editing.

Declaration of competing interest

The authors declare that they have no known competing financial interests or personal relationships that could have appeared to influence the work reported in this paper.

Acknowledgements

This study is part of the postdoctoral research of the first author, A. Bourliva, which is co-financed by Greece and the European Union (European Social Fund- ESF) through the Operational Programme "Human Resources Development, Education and Lifelong Learning" in the context of the project "Reinforcement of Postdoctoral Researchers - 2nd Cycle"

(MIS-5033021), implemented by the State Scholarships Foundation (IKY). Dr. Robert Scholger (University of Leoben, Austria) is greatly acknowledged for allowing access to the Paleomagnetic Laboratory in order to obtain part of the thermomagnetic analysis. The comments of the editor and three anonymous reviewers are highly appreciated as they improved our manuscript.

Appendix A. Supplementary data

Supplementary data to this article can be found online at https://doi.org/10.1016/j.scitotenv.2022.153600.

References

Acosta, J.A., Faz, Cano A., Arocena, J.M., Debela, F., Martínez-, Martínez S., 2009. Distribution of metals in soil particle size fractions and its implication to risk assessment of playgrounds in Murcia City (Spain). Geoderma 149, 101–109.

Ademuyiwa, O., Akinwunmi, F., Atobatele, Z., Adewole, O., Odekunle, K., Arogundade, L., Odukoya, O.O., 2013. Heavy metal burdens of public primary school children in Ibadan north-west local government area, Nigeria related to playground soils and classroom dusts. Toxicol. Lett. 28, S107–S108.

Adimalla, N., Chen, J., Qian, H., 2020. Spatial characteristics of heavy metal contamination and potential human health risk assessment of urban soils: a case study from an urban region of South India. Ecotoxicol. Environ. Saf. 194, 110406.

Aguilar-Reyes, B., Bautista, F., Goguitchaichvili, A., Morton, O., 2011. Magnetic monitoring of topsoils of Merida (Southern Mexico). Stud. Geophys. Geod. 54, 377–388.

Aidona, E., Grison, H., Petrovsky, E., Kazakis, N., Papadopoulou, L., Voudouris, K., 2016. Magnetic characteristics and trace elements concentration in soils from Anthemountas River basin (North Greece): discrimination of different sources of magnetic enhancement. Environ. Earth Sci. 75, 1375.

Akinwunmi, F., Akinhanmi, T.F., Atobatele, Z.A., Adewole, O., Odekunle, K., Arogundale, L.A., Odukoya, O.O., olayiwola O.M., Ademuyiwa O., 2017. Heavy metal burdens of public primary school children related to playground soils and classroom dusts in Ibadan north-west local government area, Nigeria. Environ. Toxicol. Pharmacol. 49, 21–26.

Aleksander-Kwaterczak, U., Rajca, A., 2015. Urban soil contamination with lead and cadmium in the playgrounds located near busy streets in Cracow (South Poland). Geol. Geophys. Environ. 41, 7–16.

Appleton, J.D., Cave, M.R., Wragg, J., 2012. Anthropogenic and geogenic impacts on arsenic bioaccessibility in UK topsoils. Sci. Total Environ. 435–436, 21–29.

Ault, A.P., Peters, T.M., Sawvel, E.J., Casuccio, G.S., Willis, R.D., Norris, G.A., Grassian, V.H., 2012. Single-particle SEM-EDX analysis of iron-containing coarse particulate matter in an urban environment: sources and distribution of iron within Cleveland, Ohio. Environ. Sci. Technol. 46, 4331–4339.

Beckwith, P.R., Ellis, J.B., Revitt, D.M., 1996. Heavy metal and magnetic relationships for urban source sediments. Phys. Earth Planet. Inter. 42, 67–75.

Blaha, U., Appel, E., Stanjek, H., 2008. Determination of anthropogenic boundary depth in industrially polluted soil and semi-quantification of heavy metal loads using magnetic susceptibility. Environ. Pollut. 156, 278–289.

Bloemendal, J., King, J.W., Hall, F.R., Doh, S.-J., 1992. Rock magnetism of late neogene and pleistocene deep-sea sediments: relationship to sediment source, diagenetic processes, and sediment lithology. J. Geophys. Res. 97, 4361–4375.

Bourliva, A., Papadopoulou, L., Aidona, E., 2016. Study of road dust magnetic phases as the main carrier of potential harmful trace elements. Sci. Total Environ. 553, 380–391.

Bourliva, A., Papadopoulou, L., Aidona, E., Giouri, K., 2017. Magnetic signature, geochemistry, and oral bioaccessibility of "technogenic" metals in contaminated industrial soils from sindos industrial area, northern Greece. Environ. Sci. Pollut. Res. 24, 17041–17055.

Bourliva, A., Kantiranis, N., Papadopoulou, L., Aidona, E., Christophoridis, C., Kollias, P., Evgenakis, M., Fytianos, K., 2018. Seasonal and spatial variations of magnetic susceptibility and potentially toxic elements (PTEs) in road dusts of Thessaloniki city, Greece: a one-year monitoring period. Sci. Total Environ. 639, 417–427.

Bourliva, A., Aidona, E., Papadopoulou, L., Ferreira da Silva, E., Patinha, C., 2021. Levels, oral bioaccessibility and health risk of sand-bound potentially harmful elements (PHEs) in public playgrounds: exploring magnetic properties as a pollution proxy. Environ. Pollut. 290, 118122.

Caboche, J., 2009. Validation d'un test de mesure de bioaccessibilité. Application à quatre éléments traces métallique dans les sols: As,Cd, Pb et Sb.L'Institut National Polytechnique de Lorraine, Nancy, p. 348 Science Agronomique. PhD

Chan, L.S., Ng, S.L., Davis, A.M., Yim, W.W.S., Yeung, C.H., 2001. Magnetic properties and heavy-metal contents of contaminated seabed sediments of Penny's bay, Hong Kong. Mar. Pollut. Bull. 42, 569–583.

Dearing, J.A., Dann, R.J.L., Hay, K., Lees, J.A., Loveland, P.J., Maher, B.A., O'Grady, K., 1996. Frequency-dependent susceptibility measurements of environmental materials. Geophys. J. Int. 124, 228–240.

Denys, S., Caboche, J., Tack, K., Rychen, G., Wragg, J., et al., 2012. In vivo validation of the unified BARGE method to assess the bioaccessibility of arsenic, antimony, cadmium, and lead in soils. Environ. Sci. Technol. 46, 6252–6260.

Dunlop, D.J., 2002. Theory and application of the Day plot (Mrs/Ms versus Hcr/Hc) 1. Theoretical curves and tests using titanomagnetite data. Journal of Geophysical Research: Solid Earth 107, EPM4-1–EPM4-22.

Dunlop, D.J., 2014. High-temperature susceptibility of magnetite: a new pseudo-single-domain effect. Geophys. J. Int. 199, 707–716.

Dytłow, S., Winkel, A., Górka-Kostrubiec, B., Sagnotti, L., 2019. Magnetic, geochemical and granulometric properties of street dust from Warsaw (Poland). J. Appl. Geophys. 169, 58–73.

Farmer, J.G., Broadway, A., Cave, M.R., Wragg, J., Fordyce, F., Graham, M.C., Ngwenya, B.T., Bewley, R.J.F., 2011. A lead isotopic study of the human bioaccessibility of lead in urban soils from Glasgow, Scotland. Sci. Total Environ. 409, 4958–4965.

Guney, M., Zagury, G.J., Dogan, N., Onay, T.T., 2010. Exposure assessment and risk characterization from trace elements following soil ingestion by children exposed to playgrounds, parks and picnic areas. J. Hazard. Mater. 182, 656–664.

Guo, B., Su, Y., Pei, L., Wang, X., Zhang, B., Zhang, D., Wang, X., 2020. Ecological risk evaluation and source apportionment of heavy metals in park playgrounds: a case study in Xi'an, Shaanxi Province, a northwest city of China. Environ. Sci. Pollut. Res. 27, 24400–24412.

Halsall, C.J., Maher, B.A., Karloukovski, V.V., Shah, P., Watkins, S.J., 2008. A novel approach to investigating indoor/outdoor pollution links: combined magnetic and PAH measurements. Atmos. Environ. 42, 8902–8909.

Hamilton, E.M., Barlow, T.S., Gowing, C.J.B., Watts, M.J., 2015. Bioaccessibility performance data for fifty-seven elements in guidance material BGS 102. Microchem. J. 123, 131–138.

Heidari, M., Darijani, T., Alipour, V., 2021. Heavy metal pollution of road dust in a city and its highly polluted suburb; quantitative source apportionment and source-specific ecological and health risk assessment. Chemosphere 273, 129656.

Heider, F., Zitzelsberger, A., Fabian, K., 1996. Magnetic susceptibility and remanent coercive force in grown magnetite crystals from 0.1 μm to 6 mm. Phys. Earth Planet. Inter. 93, 239–256.

Hiller, E., Filová, L., Jurkovič, L., Lachká, L., Kulikova, T., Šimurková, M., 2018. Arsenic in playground soils from kindergartens and green recreational areas of Bratislava City (Slovakia): occurrence and gastric bioaccessibility. Arch. Environ. Contam. Toxicol. 75, 402–414.

Hiller, E., Filová, L., Jurkovič, E., Mihaljevič, M., Lachká, L., Rapant, S., 2020. Trace elements in two particle size fractions of urban soils collected from playgrounds in Bratislava (Slovakia). Environ. Geochem. Health 42, 3925–3947.

Hu, X.-F., Su, Y., Ye, R., Li, X.-Q., Zhang, G.-L., 2007. Magnetic properties of the urban soils in Shanghai and their environmental implications. Catena 70, 428–436.

ISO 17924, 2018. Soil Quality—Assessment of Human Exposure from Ingestion of Soil and Soil Material—Procedure for the Estimation of the Human Bioaccessibility/Bioavailability of Metals in Soil. 2018. ISO, Genève, Switzerland.

Javed, S.A., Al-Bratty, M., Al-Rajab, A.J., Alhazmi, H.A., Ahsan, W., Abdelwahab, S.I., Thangavel, N., 2019. Risk-based exposure assessment for multiple toxic elements encountered by children in school playgrounds and parks in the southwest region of Saudi Arabia. Environ. Monit. Assess. 191, 549.

Jeleńska, M., Hasso-Agopsowicz, A., Kopcewicz, B., Sukhorada, A., Tyamina, K., Kadziałko-Hofmokl, M., Matviishina, Z., 2004. Magnetic properties of the profiles of polluted and non-polluted soils. A case study from Ukraine. Geophys. J. Int. 159, 104–116.

Jin, Y., O'Connor, D., Ok, Y.S., Tsang, D.C.W., Liu, A., Hou, D., 2019. Assessment of sources of heavy metals in soil and dust at children's playgrounds in Beijing using GIS and multivariate statistical analysis. Environ. Int. 124, 320–328.

Kelepertzis, E., Argyraki, A., Botsou, F., Aidona, E., Szabó, A., Szabó, C., 2019. Tracking the occurrence of anthropogenic magnetic particles and potentially toxic elements (PTEs) in house dust using magnetic and geochemical analyses. Environ. Pollut. 245, 909–920.

Kelepertzis, E., Chrastný, V., Botsou, F., Sigala, E., Kypritidou, Z., Kamárek, M., Skordas, K., Argyraki, A., 2021. Tracing the sources of bioaccessible metal(loid)s in urban environments: a multidisciplinary approach. Science of the Total Environment 771, 144827.

Kim, W., Doh, S.-J., Park, Y.-H., Yun, S.-T., 2007. Two-year magnetic monitoring in conjunction with geochemical and electron microscopic data of roadside dust in Seoul, Korea. Atmos. Environ. 41, 7627–7641.

Kim, W., Suh, C.-Y., Cho, S.-W., Roh, K.-M., Kwon, H., Song, K., Shon, I.-J., 2012. A new method for the identification and quantification of magnetite–maghemite mixture using conventional X-ray diffraction technique. Talanta 94, 348–352.

Kim, E.J., Yoo, J.C., Baek, K., 2014. Arsenic speciation and bioaccessibility in arsenic-contaminated soils: sequential extraction and mineralogical investigation. Environ. Pollut. 186, 29–35.

Laha, T., Gope, M., Datta, S., Masto, R.E., Balachandran, S., 2020. Oral bioaccessibility of potentially toxic elements (PTEs) and related health risk in urban playground soil from a medieval bell metal industrial town Khagra, India. Environmental Geochemistry and Health https://doi.org/10.1007/s10653-020-00715-y.

Lecoanet, H., Léveque, F., Ambrosi, J.-P., 2003. Combination of magnetic parameters: an efficient way to discriminate soil-contamination sources (south France). Environ. Pollut. 122, 229–234.

Li, H., Qian, X., Wei, H., Zhang, R., Yang, Y., Liu, Z., Hu, W., Gao, H., Wang, Y., 2014. Magnetic properties as proxies for the evaluation of heavy metal contamination in urban street dusts of Nanjing, Southeast China. Geophys. J. Int. 199, 1354–1366.

Li, M., Zhu, S., Ouyang, T., Tang, J., Tang, Z., 2021. Magnetic properties of the surface sediments in the Yellow River estuary and Laizhou Bay, Bohai Sea, China: implications for monitoring heavy metals. J. Hazard. Mater. 410, 124579.

Liu, P., Hu, W., Tian, K., Huang, B., Zhao, Y., Wang, X., Zhou, Y., Shi, B., Kwon, B.-O., Choi, K., Ryu, J., Chen, Y., Wnag, T., Khim, J.S., 2020. Accumulation and ecological risk of heavy metals in soils along the coastal areas of the Bohai Sea and the Yellow Sea: a comparative study of China and South Korea. Environ. Int. 137, 105519.

Liu, H., Yan, Y., Chang, H., Chen, H., Liang, L., Liu, X., Qiang, X., Sun, Y., 2019. Magnetic signatures of natural and anthropogenic sources of urban dust aerosol. Atmos. Chem. Phys. 19, 731–745.

Ljung, K., Selinus, O., Otabbong, E., 2006. Metals in soils of children's urban environments in the small northern european city of Uppsala. Sci. Total Environ. 366, 749–759.

Lu, S.G., Bai, S.Q., 2006. Study on the correlation of magnetic properties and heavy metals content in urban soils of Hangzhou City, China. J. Appl. Geophys. 60, 1–12.

Łukasik, A., Szuszkiewicz, M., Magiera, T., 2014. Impact of artifacts on topsoil magnetic susceptibility enhancement in urban parks of the upper Silesian conurbation datasets. J. Soils Sediments 15, 1836–1846.
Magiera, T., Strzyszcz, Z., Rachwal, M., 2007. Mapping particulate pollution loads using soil magnetometry in urban forests in the Upper Silesia Industrial Region, Poland. For. Ecol. Manag. 248, 36–42.
Magiera, T., Jabłońska, M., Strzyszcz, Z., Rachwal, M., 2011. Morphological and mineralogical forms of technogenic magnetic particles in industrial dusts. Atmos. Environ. 45, 4281–4290.
Maher, B.A., 1988. Magnetic properties of some synthetic sub-micron magnetites. Geophys. J. 94, 83–96.
Maher, B.A., Ahmed, I.A., Karloukovski, V., MacLaren, D.A., Foulds, P.G., Allsop, D., Manne, D.M.A., Torres-Jardón, R., Calderon-Garciduenas, L., 2016. Magnetite pollution nanoparticles in the human brain. Proc.Natl. Acad. Sci. U. S. A. 113, 10797–10801.
Massas, I., Ehaliotis, C., Kalivas, D., Panagopoulou, G., 2010. Concentrations and availability indicators of soil heavy metals; the case of children's playgrounds in the city of Athens (Greece). Water Air Soil Pollut. 212, 51–63.
Meza-Figueroa, D., Barboza-Flores, M., Romero, F.M., Acosta-Elias, M., Hernández-Mendiola, E., Maldonado-Escalante, F., et al., 2020. Metal bioaccessibility, particle size distribution and polydispersity of playground dust in synthetic lysosomal fluids. Sci. Total Environ. 713, 136481.
de Miguel, E., Iribarren, I., Chacón, E., Ordonez, A., Charlesworth, S., 2007. Evaluation of the exposure of children to trace elements in playgrounds in Madrid (Spain). Chemosphere 66, 505–513.
Ng, S.L., Chan, L.S., Lam, K.C., Chan, W.K., 2003. Heavy metal contents and magnetic properties of playground dust in Hong-Kong. Environ. Monit. Assess. 89, 221–232.
Ottesen, R.T., Alexander, J., Langedal, M., Haugland, T., Høygaard, E., 2008. Soil pollution in day-care centers and playgrounds in Norway: national action plan for mapping and remediation. Environ. Geochem. Health 30, 623–637.
Palumbo-Roe, B., Wragg, J., Cave, M., 2015. Linking selective chemical extraction of iron oxyhydroxides to arsenic bioaccessibility in soil. Environ. Pollut. 207, 256–265.
Peng, T., O'Connor, D., Zhao, B., Jin, Y., Zhang, Y., Tian, L., Zheng, N., Li, X., Hou, D., 2019. Spatial distribution of lead contamination in soil and equipment dust at children's playgrounds in Beijing, China. Environ. Pollut. 245, 363–370.
Ramazanova, E., Lee, S.H., Lee, W., 2021. Stochastic risk assessment of urban soils contaminated by heavy metals in Kazakhstan. Sci. Total Environ. 750, 141535.
Reis, A.P., Patinha, C., Wragg, J., Dias, A.C., Cave, M., Sousa, A.J., Batista, M.J., Prazeres, C., Costa, C., Ferreira da Silva, E., Rocha, F., 2014. Urban geochemistry of lead in gardens, playgrounds and schoolyards of Lisbon, Portugal: assessing exposure and risk to human health. Appl. Geochem. 44, 45–63.
Rodriguez-Oroz, D., Vidal, R., Fernandoy, F., Lambert, F., Quiero, F., 2018. Metal concentrations and source identification in Chilean public children's playgrounds. Environ. Monit. Assess. 190, 703.
Rózański, S.Ł., Kwasowski, W., Castejón, J.M.P., Hardy, A., 2018. Heavy metal content and mobility in urban soils of public playgrounds and sport facility areas, Poland. Chemosphere 212, 456–466.
Sapcanin, A., Cakal, M., Jacimovic, Z., Pehlic, E., Jancan, G., 2017. Soil pollution fingerprints of children playgrounds in Sarajevo city, Bosnia and Herzegovina. Environ. Sci. Pollut. Res. 24, 10949–10954.
Schmidt, A., Yarnold, R., Hill, M., Ashmore, M., 2005. Magnetic susceptibility as proxy for heavy metal pollution: a site study. J. Geochem. Explor. 85, 109–117.
Shahab, A., Zhang, H., Ullah, H., Rashid, A., Rad, S., Li, J., Xiao, H., 2020. Pollution characteristics and toxicity of potentially toxic elements in road dust of a tourist city, Guilin, China: ecological and health risk assessment. Environ. Pollut. 266, 115419.
Shilton, V.F., Booth, C.A., Smith, J.P., Giess, P., Mitchell, D.J., Williams, C.D., 2005. Magnetic properties of urban street dust and their relationship with organic matter content in the west midlands, UK. Atmos. Environ. 39, 3651–3659.
Song, Y., Wang, X., Maher, B.A., Li, F., Xu, C., Liu, X., Sun, X., Zhang, Z., 2016. The spatial-temporal characteristics and health impacts of ambient fine particulate matter in China. J. Clean. Prod. 112, 1312–1318.
Szuszkiewicz, M., Magiera, T., Kapička, A., Grison, H., Gołuchowska, B., Petrovský, E., 2015. Magnetic characteristics of industrial dust from different sources of emission: a case study of Poland. Journal of Applied Geophysics 116, 84–92.
Thompson, R., Oldfield, F., 1986. Environmental Magnetism. Allen and Unwin, London.
Valido, I.H., Padoan, E., Moreno, T., Querol, X., Font, O., Amato, F., 2018. Physico-chemical characterization of playground sand dust, inhalable and bioaccessible fractions. Chemosphere 190, 454–462.
Wang, X.S., 2013. Magnetic properties and heavy metal pollution of soils in the vicinity of a cement plant, Xuzhou (China). J. Appl. Geophys. 98, 73–78.
Wang, G., Oldfield, F., Xia, D., Chen, F., Liu, X., Zhang, W., 2012. Magnetic properties and correlation with heavy metals in urban street dust: a case study from the city of Lanzhou, China. Atmos. Environ. 46, 289–298.
Wang, B., Xia, D.S., Yu, Y., Jia, J., Xu, S., 2013. Magnetic records of heavy metal pollution in urban topsoil in Lanzhou, China. Chin. Sci. Bull. 58, 384–395.
Wang, B., Xia, D., Yu, Y., Jia, J., Xu, S., 2014. Detection and differentiation of pollution in urban surface soils using magnetic properties in arid and semi-arid regions of northwestern China. Environ. Pollut. 184, 335–346.
Wang, G., Ren, F., Chen, J., Liu, Y., Ye, F., Oldfield, F., Zhang, W., Zhang, X., 2017. Magnetic evidence of anthropogenic dust deposition in urban soils of Shanghai, China. Chem. Erde 77, 421–428.
Wang, G., Chen, J., Zhang, W., Chen, Y., Ren, F., Fang, A., Ma, L., 2019a. Relationship between magnetic properties and heavy metal contamination of street dust samples from Shanghai, China. Environ. Sci. Pollut. Res. 26, 8958–8970.
Wang, G., Chen, J., Zhang, W., Ren, F., Chen, Y., Fang, A., Ma, L., 2019b. Magnetic properties of street dust in Shanghai, China and its relationship to anthropogenic activities. Environ. Pollut. 255, 113214.
Wills, B.A., Finch, J.A., 2016. Magnetic and electrical separation. Wills' Mineral Processing Technology. Butterworth-Heinemann, pp. 381–407.
Wragg, J., Cave, M., Nathanail, P., 2007. A study of the relationship between arsenic bioaccessibility and its solid-phase distribution in soils from Wellingborough, UK. J. Environ. Sci. Health Part A 42, 1303–1315.
Xia, D., Wang, B., Yu, Y., Jia, J., Nie, Y., Wang, X., Xu, S., 2014. Combination of magnetic parameters and heavy metals to discriminate soil-contamination sources in Yinchuan - a typical oasis city of northwestern China. Sci. Total Environ. 485–486, 83–92.
Xie, S., Dearing, J.A., Bloemendal, J., Boyle, J.F., 1999. Association between the organic matter content and magnetic properties in street dust, Liverpool, UK. Sci. Total Environ. 241, 205–214.
Xie, S., Dearing, J.A., Bloemandal, J., 2000. The organic matter content of street dust in Liverpool, UK, and its association with dust magnetic properties. Atmos. Environ. 34, 269–275.
Xie, S., Dearing, J.A., Boyle, J.F., Bloemendal, J., Morse, A.P., 2001. Association between magnetic properties and element concentrations of Liverpool street dust and its implications. J. Appl. Geophys. 48, 83–92.
Yang, M., Li, H.-M., Li, F.-Y., Wang, J.-H., Diao, Y.-W., Qian, X., Yang, Z.-P., Wang, C., 2017. Magnetic response of heavy metal pollution in playground dust of an industrial area. Huanjing Kexue 38, 5282–5291.
Yang, D., Wu, J., Hong, H., Liu, J., Yan, C., Lu, H., 2021. Traffic-related magnetic pollution in urban dust from the Xiamen Island, China. Environmental Chemistry Letters https://doi.org/10.1007/s10311-021-01270-3.
Zgłobicki, W., Telecka, M., Skupiński, S., 2020. Heavy metals in playgrounds in Lublin (E Poland): sources, pollution levels and health risk. Environ. Sci. Pollut. Res. https://doi.org/10.1007/s11356-020-09375-y in press.
Zhao, G., Zhang, R., Han, Y., Lu, B., Meng, Y., Wang, S., Wang, N., 2020. Identifying environmental pollution recorded in street dust using the magnetic method: a case study from central eastern China. Environmental Science and Pollution Research 27, 34966–34977.
Zheng, Y., Zhang, S.-H., 2008. Magnetic properties of street dust and topsoil in Beijing and its environmental implications. Chin. Sci. Bull. 53, 408–417.
Zhu, Z., Han, Z., Bi, X., Yang, W., 2012. The relationship between magnetic parameters and heavy metal contents of indoor dust in e-waste recycling impacted area, Southeast China. Sci. Total Environ. 433, 302–308.